Climate Modelling User Group

Deliverable D2.0e

Interim report on progress achieved in WP5.5: Cloud and Aerosol Analysis Study

Centres providing input: ECMWF, BSC

Version nr.	Date	Status
0.1	29 February 2024	First draft
0.2	28 February 2024	ECMWF update on WP 5.5.2
0.3	29 February 2024	BSC update on WP 5.5.1
1.0	29 February 2024	Submitted to CMUG PI
1.1	08 March 2024	Submitted to ESA
1.2	18 March 2024	Submitted to ESA with corrections

CMUG CCI+ Deliverable D2.0e

Interim report on progress achieved in WP5.5

Table of Contents

Interim report on progress achieved in WP5.5

1. Purpose and scope of this report

This document is the first interim report on activities carried on in the WP5.5 Clouds and Aerosol study CMUG-CCI+. The aim of the study is to exploit ESA CCI and CCI+ data of aerosols and clouds for assimilation in Earth System Models. For this purpose, we use two ECVs, clouds and aerosols, and two different models and approaches for the assimilation. ECMWF assimilates operationally, in their 4D-Var system, aerosol optical depth in the Copernicus Atmosphere Monitoring Service for atmospheric composition forecasts, while limited cloud information is assimilated for Numerical Weather Prediction and reanalyses. This study proposes to assimilate both, aerosols and cloud information synergistically in the 4D-Var system.

BSC produces operationally daily forecasts of dust in the WMO Barcelona Dust Regional Centre. It expects to produce forecasts with dust assimilation with an ensemble LETKF assimilation scheme in the next model upgrade, scheduled for Q4 of this year. Dedicated dust observations are essential for this application, as well as for the constraint of the dust cycle in the Earth system. Using satellite dust optical depth, the MONARCH model at BSC has produced a 10-years dust reanalysis (Di Tomaso et al. 2022), which has been recently extended for one more year. This work will assess the potential benefit of using most recent developments on CCI aerosol retrievals for dust data assimilation, with perspectives of being used for assimilation in future dust reanalysis, and for verification of past operational forecasts.

We report here the progress about the following:

1. Initial assessment of the impact of Cloud Optical Depth (COD) and Aerosol Optical Depth (AOD) level 2 data on the 4D-Var analysis both for air quality fields and for meteorological variables
2. Initial assessment of the impact of coarse mode AOD to constrain desert dust simulations

2. Progress on the tasks

2.1. Progress on WP5.5.1: Dust aerosol analysis in the BSC system

Lead partner: BSC
Authors: Jeronimo Escribano, Eleni Karnezi, Emanuele Emili and Calum Meikle

Preliminary work and overview

The CMUG study follows up part of the work performed during the ESA's DOMOS project. During DOMOS, three experiments were performed: (i) assimilation of AOD from VIIRS Deep Blue, version 1 from Suomi-NPP (SNPP), filtered by retrieval flag of "dust"; (ii) Assimilation of dust extinction coefficient from the LIVAS product, based on CALIOP profiles, and (iii) joint assimilation of LIVAS and VIIRS data. Hence, WP5.5.1 experiments can be directly compared to those of DOMOS. This allows to fully exploit their outcomes, and sets a baseline for the evaluation of WP5.5.1 results. That said, this task will explore the assimilation of CCI data for the same case of study and using the same verifications scores and tools.

WP5.5.1 will assimilate the v1.14 of SLSTR aerosol optical depth, produced by Swansea University, during the Godzilla dust event in June 2020.

Visual inspection of SLSTR aerosol optical depth retrievals for June 2020

Sentinel3A and Sentinel3B SLSTR aerosol retrievals, level 2 and level 3, were kindly provided by Peter North and Kevin Pearson for this study. We assimilate level 2 retrievals, while we use level 3 retrievals for easy visual inspection of the values. Figure 1 shows snapshots of 18UTC instantaneous values of MONARCH's mineral dust optical depth (DOD) control run, their coarse contribution to the dust optical depth, SLSTR-A and SLSTR-B daily averaged retrievals of total AOD, dust AOD and coarse AOD, VIIRS DOD filtered from Deep Blue SNPP retrievals, and finally the coarse DOD from VIIRS retrievals applying to VIIRS the algorithm for dust filtering, described in Pu and Ginoux (2016).

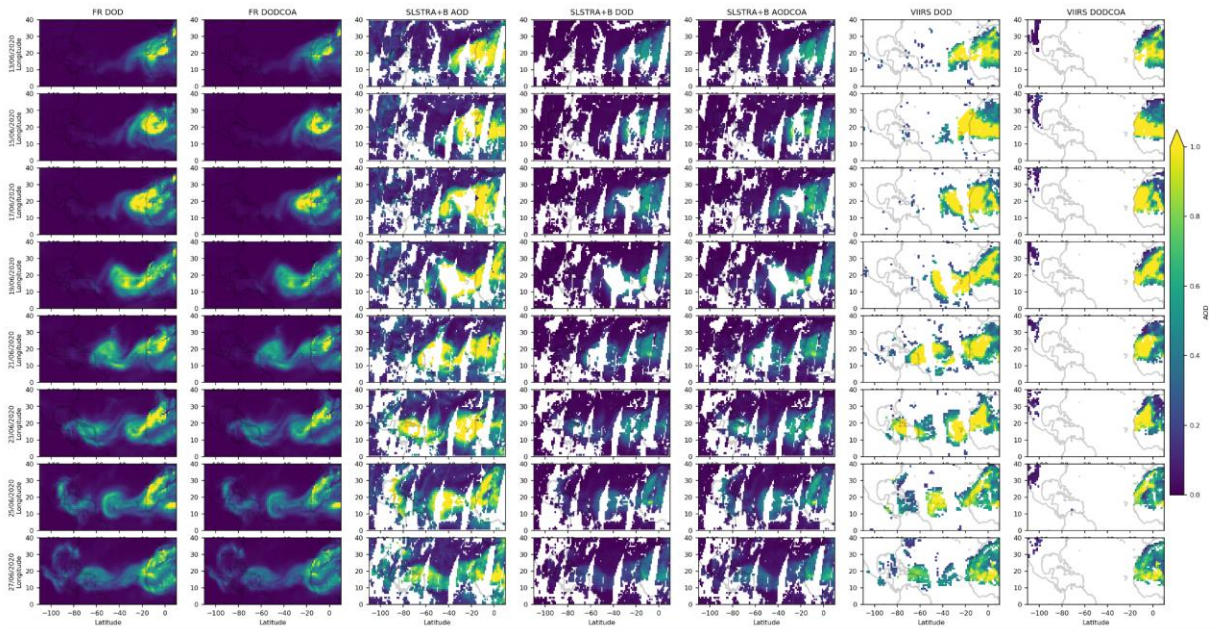

Figure 1: Model and satellite retrievals aerosol information from 18UTC June 13 (top row) to 18UTC June 27(bottom row) in two day time steps. Columns: Control model run AOD, Control model run coarse AOD, SLSTR AOD, SLSTR dust AOD, SLSTR coarse AOD, VIIRS SNPP dust AOD, VIIRS SNPP coarse Dust AOD.

Figure 1 shows the dust plume moving westward over the Atlantic Ocean in the model run without assimilation (as FR stands for "free run"), and both retrievals over the Atlantic Ocean SLSTR and VIIRS. The overall structure of the dust plume is well noticed in the total AOD SLSTR retrievals, and they are similar to the filtered AOD retrievals from VIIRS. MONARCH simulations also show the structure of the dust plume, but with lower values of DOD. Collocated comparisons between the model runs without assimilation and SLSTR products are shown in Figure 2. These plots show that total AOD from SLSTR (and dust filtered AOD from VIIRS) are larger than the MONARCH control run while both, coarse AOD and DOD from SLSTR, are lower than the model control run, especially for larger values of model DOD.

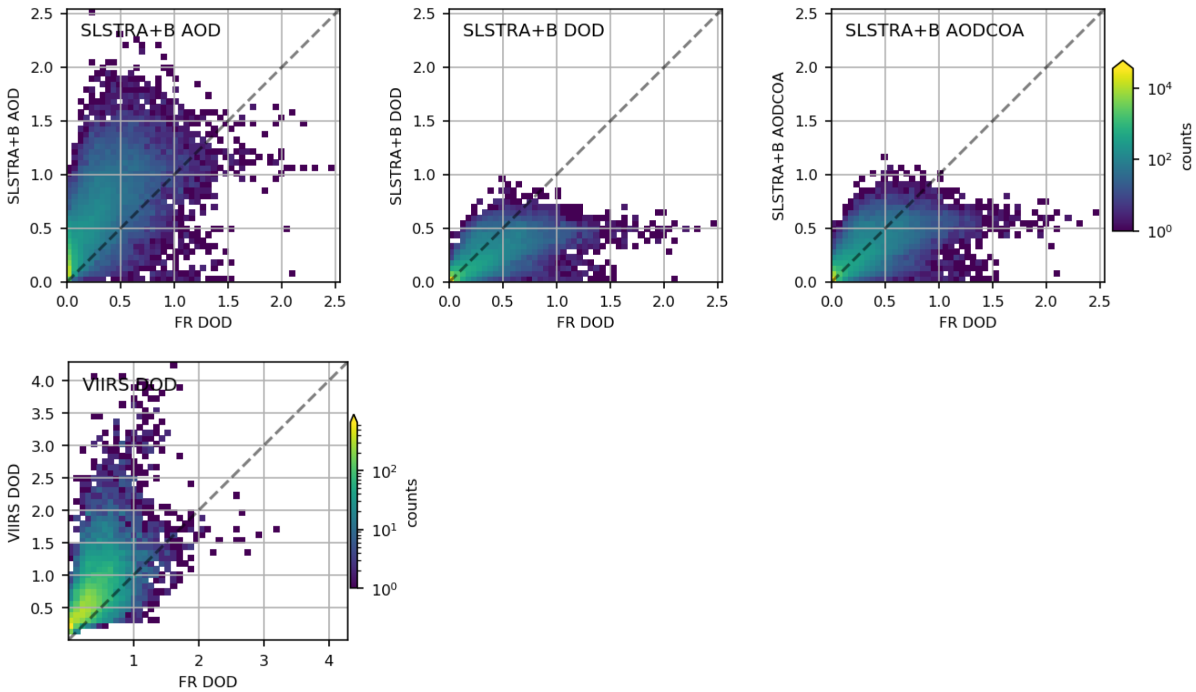

Figure 2: Bidimensional histograms for collocated control run DOD (x-axis), SLSTR products (y-axis, top row) and VIIRS DOD (y-axis, bottom row).

The ratio between the coarse to total dust is also different in the model than in SLSTR products. Figure 3 shows in the first column the DOD of the model, and in the second column the ratio between coarse to total model DOD. Equivalent ratio is shown in the last column for coarse to total AOD of SLSTR, being the total AOD in the third column of Figure 3. MONARCH model shows a ratio of coarse DOD (DODCOA) to DOD of about 0.75 to 0.8 over the dust plume, while in SLSTR retrievals the ratio of coarse AOD to AOD is between 0.3 to 0.7. It is known that dust models underestimate the coarse dust in the atmosphere (Adebiyi et al. 2023), and because the model ratio is larger than the SLSTR ratio, this suggests an underestimation of SLSTR coarse contribution to the total AOD for this dust event over the Atlantic Ocean.

The SLSTR dust to total AOD product show even lower values than the ratio of coarse to total (dust over coarse AOD is lower than 1, in the fifth row of Figure 3). All in all, any assimilation of a biased low DOD or coarse AOD into an already underestimated DOD from MONARCH will decrease the DOD values of MONARCH analysis, increasing the bias and worsening the skill scores. In the following and to showcase the potential of assimilation of CCI SLSTR data in the MONARCH system, we show an assimilation experiment using total AOD instead of DOD retrievals. Because the Godzilla dust event signal is unique and strong over the Atlantic Ocean compared with other aerosols in this scene, and because the model ensemble spread away from the dust plume is small (because model DOD values there are also small), the following approximation which does not distinguish between AOD and DOD in this case is not critical. In a more general situation (operational DOD assimilation for example), this assumption can lead to a considerable degradation of the forecast and analysis skills.

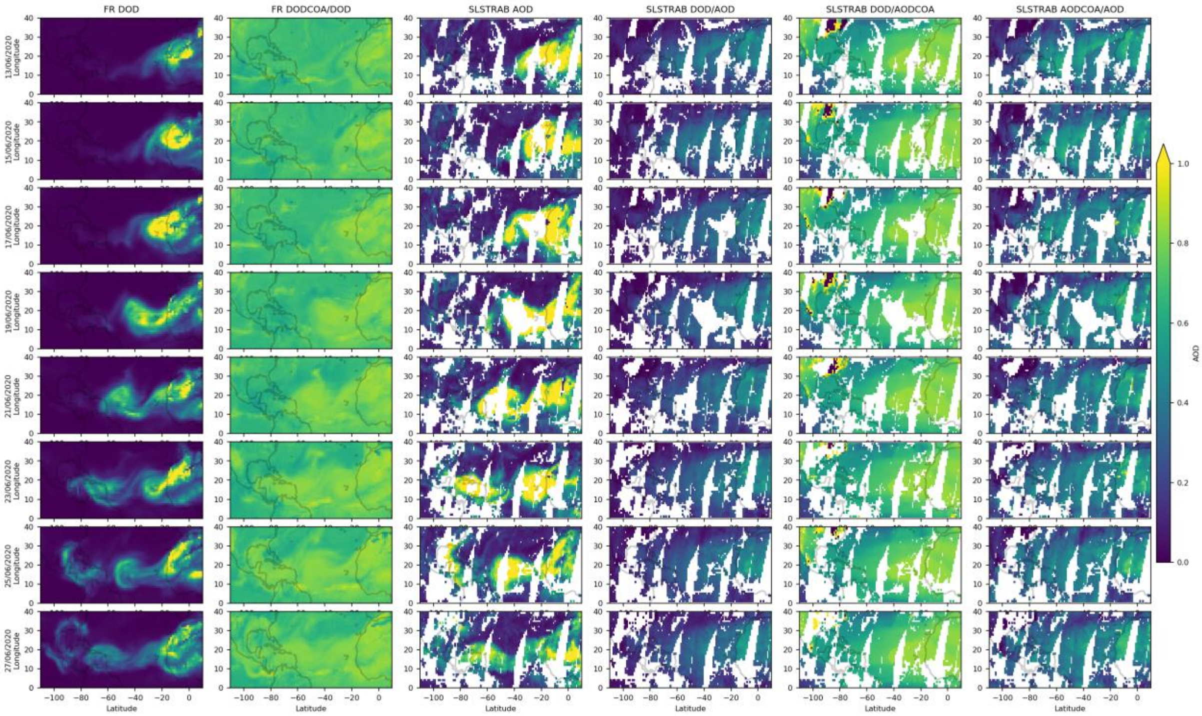

Figure 3: Ratio of dust AOD or coarse AOD to the total AOD or DOD. Columns: Control model run DOD, Control model run ratio of coarse AOD/DOD, SLSTR AOD, SLSTR ratio of DOD/AOD, SLSTR ratio of DOD/coarse AOD and SLSTR ratio of coarse AOD/AOD.

SLSTR AOD assimilation in MONARCH LETKF

We have prepared and run the MONARCH assimilation system for the Godzilla event in June 2020. MONARCH model was configured in a global domain (it can also run in limited area model configuration), with an ensemble of 20 members, and horizontal resolution of 1.4 degrees in longitude and 1 degree in latitude. Dust emissions configuration settings are like G01 of Klose et al. (2022), and dust-radiation interaction is switched on. Perturbations for these members are similar to those of Escribano et al. (2022), that is, using meteorological initial conditions from the 20 members GEFS forecasts (produced in 2020), and dust source strength factors with bidimensional maps of 250 km correlated Gaussian noise with mean of 1 and standard deviation of 0.2. For the assimilation, we have used the Local Ensemble Kalman Filter (LETKF, Hunt et al. 2007) in their 4D extension version. The assimilation window is of 24-hours starting a 0 UTC. Localization is done with a gaussian function in the observational space. The horizontal localization length scale is set to 4 model grid points, while the temporal localization is set to 12 hours. The observation operator interpolates the model ensemble to the level 2 satellite retrievals locations in space, within the hourly instantaneous resolution of the model outputs. Observation operator error is added to the system with a constant value of 0.02 in AOD.

As indicated in the previous section, we assimilated AOD from level 2, version 1.14 SU SLSTR retrievals from Sentinel-3A and Sentinel-3B. We perform two experiments assimilating the same AOD data. A first experiment, called SLSTR-linear, assumes a linear model for the uncertainty of the assimilated AOD (uncertainty = 0.2*AOD + 0.05). This assumption (originally from MODIS DT validation studies) is commonly used in aerosol data assimilation, and it allows to compare the experiment with for example, the VIIRS assimilation experiment performed in DOMOS that assumes the same model for the uncertainty. A second experiment, called SLSTR-pixel, makes use of the reported pixel-level uncertainties in the data assimilation system. A direct comparison between both experiments can provide useful information on the best use of these uncertainty estimates.

Figure 4 shows the two analyses of using SLSTR data. The first column shows the control run, that is, MONARCH run without assimilation and the columns AN LIN_UNC and AN PIX_UNC shows the analysis after the assimilation of SLSTR with the two uncertainties estimates. As for reference, the analysis produced with VIIRS assimilation are shown in the last column. For the latter, we use the same linear model of uncertainties with that for SLSTR.

SLSTR assimilation can increment DOD values of the dust plume in the model and can produce a similar plume as the VIIRS analysis. This increment is done even in situations where the SLSTR retrievals are not reported, as for example the centre of the plume on 19 of June (4th column, 4th row). The pixel level uncertainty experiment shows larger DOD values in the analysis, and a distinct small-scale structure. This might be investigated in the future. On the contrary, SLSTR linear uncertainty experiment behaves like VIIRS analysis.

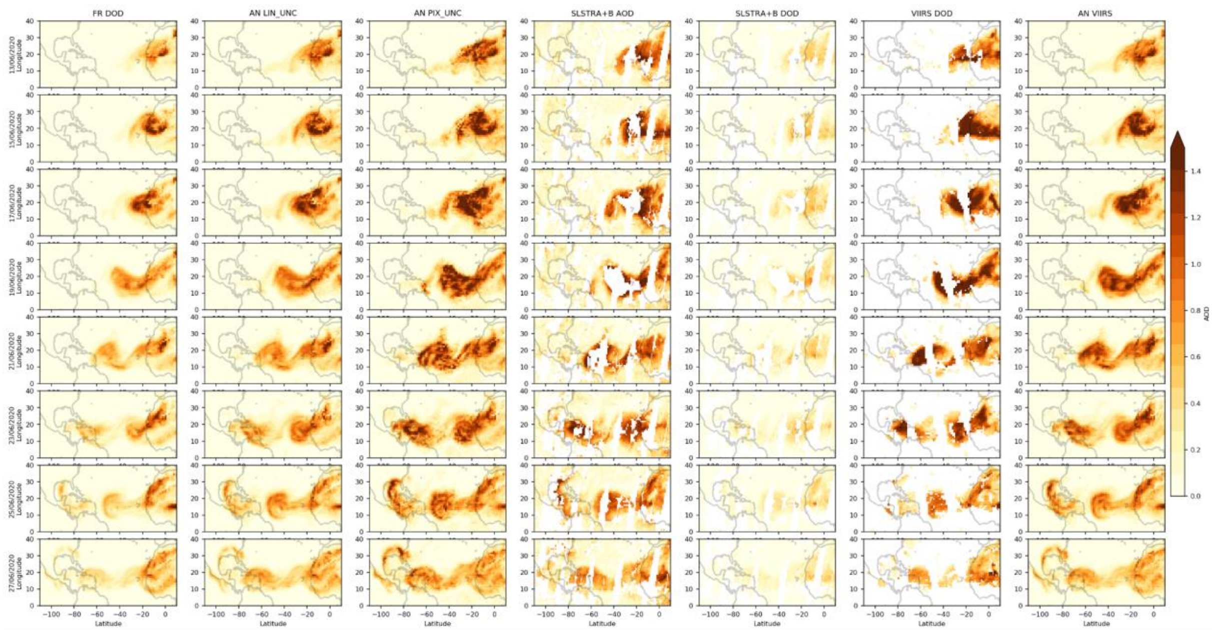

Figure 4: Assimilation of SLSTR AOD. Snapshots of simulated (18UTC) dust optical depth and satellite retrievals. Columns are: model control run, analysis of the linear uncertainty

experiment, analysis of the pixel-level uncertainty, averaged SLSTR AOD, averaged SLSTR DOD, VIIRS DOD and analysis of the VIIRS experiment.

Although a proper verification is planned in OWP5.5, we show in the following figures the comparison of the analysis with the coarse AOD retrieval from AERONET O'Neill product. For the domain of interest, the overall skill scores improve after SLSTR assimilation in comparison to the control run (FR), as shown in shown in Table 1 and the associated time-series of Figure 5. Moreover, bias ("mean" in the table), RMSE, Mean Fractional Bias and Mean Fractional Error shows best values among all experiments for the assimilation of SLSTR with pixel uncertainties.

Table 1: Verification scores for all AERONET stations in the period. "mean" column of the right table indicates the mean bias of the experiment.

	Mean	StdDev	p5	Median	p95
observations	0.20	0.31	0.01	0.07	1.00
FR	0.08	0.12	0.00	0.02	0.36
LIVAS	0.11	0.18	0.00	0.03	0.54
LIVAS+VIIRS	0.14	0.20	0.00	0.04	0.62
VIIRS	0.13	0.20	0.00	0.03	0.61
SLSTR-linear	0.11	0.16	0.00	0.04	0.48
SLSTR-pixel	0.17	0.22	0.00	0.06	0.66

	Mean	RMSE	r	MFB	MFE
FR	-0.12	0.25	0.81	-100.02	111.68
LIVAS	-0.08	0.21	0.82	-80.44	100.16
LIVAS+VIIRS	-0.06	0.17	0.89	-62.02	88.64
VIIRS	-0.06	0.17	0.90	-69.32	92.23
SLSTR-linear	-0.08	0.22	0.83	-67.27	90.46
SLSTR-pixel	-0.03	0.17	0.86	-33.29	75.76

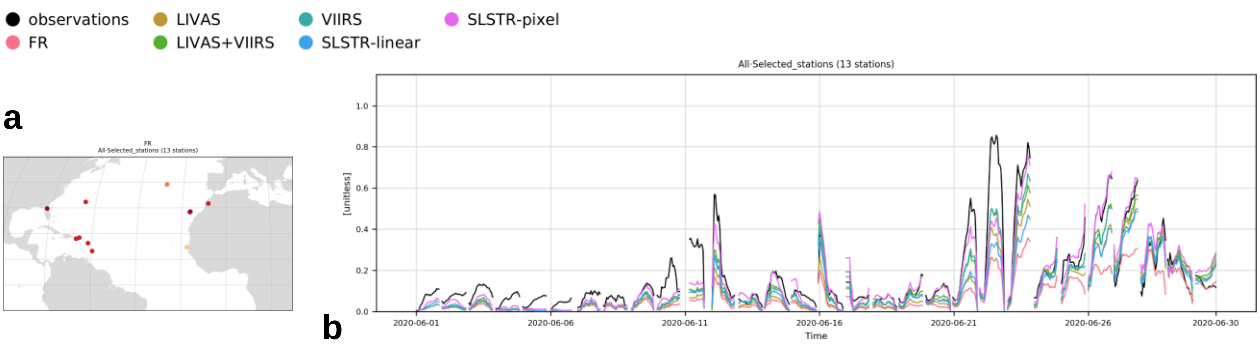

Figure 5: a) Map of location of the 13 stations included in the study. b) Spatially averaged time-series of coarse AOD AERONET retrievals and MONARCH DOD coarse analyses.

We also show the time-series and associated skill scores for 3 stations across the Atlantic in Figure 6. From east to west: Ragged Point in Barbados, La Parguera in Puerto Rico and NEON OSBS in the United States (Florida). In these three sites, the Godzilla plume is observed as the maximum peak of the black lines. In agreement with Figure 5, SLSTR analyses show improvement in the skills, and the experiment that uses pixel uncertainties produces remarkable scores in almost all sites.

We note that the control run is biased low in comparison with AERONET for these sites. Also, it is known that SLSTR AOD can be (globally) biased high. In addition, the assumption of confounding AOD and DOD in the assimilation imposes a high bias of the assimilated observations. Therefore, it should not be discarded that the improvement in the analysis scores is due to the assimilation of biased observations, that counteracts the low biased control model run, thus improving RMSE, MFE, MFB scores but not substantially the linear correlation.

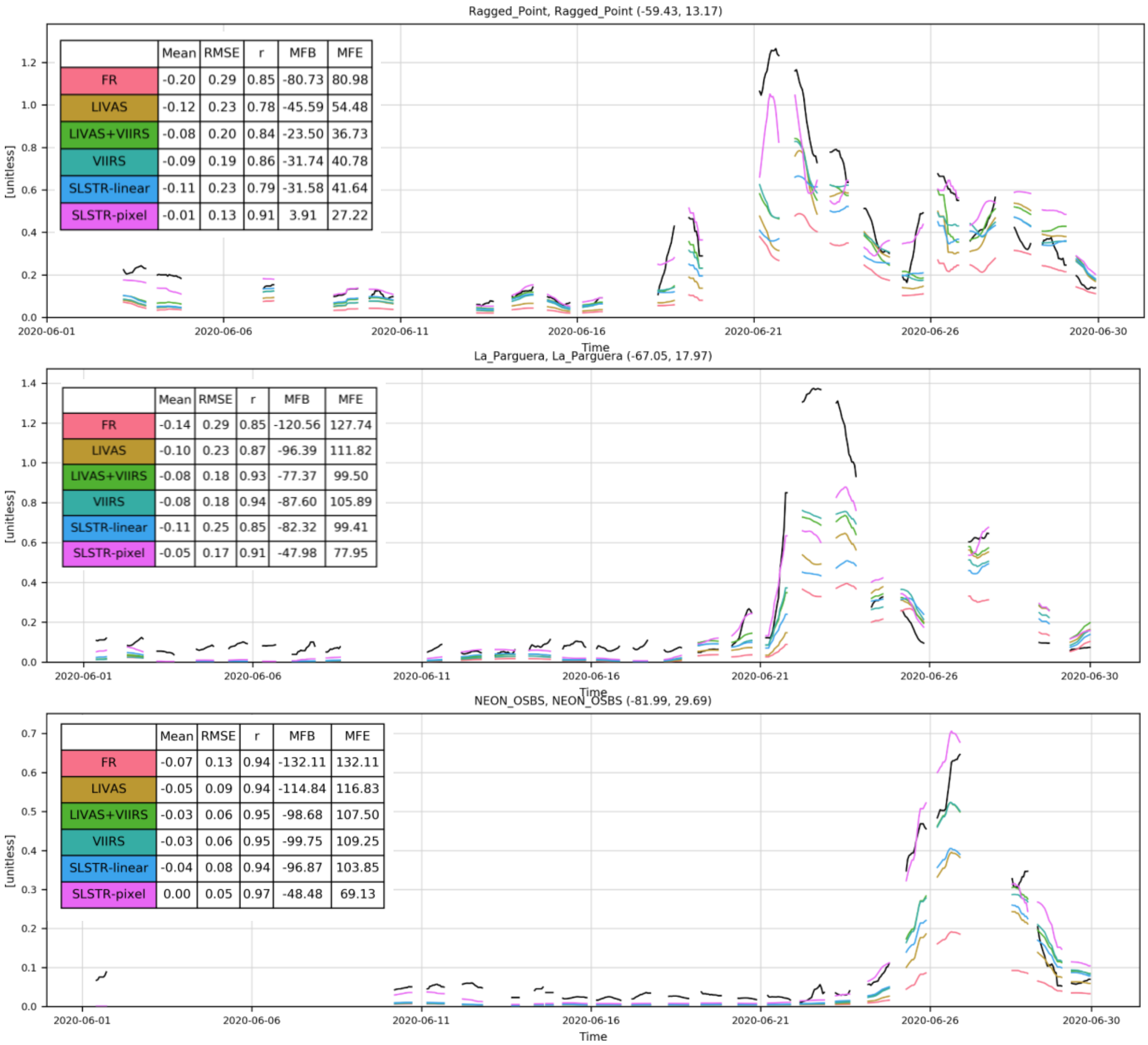

Figure 6: Time-series of coarse AOD for three sites in the in the Caribbean and the US.

Similarly, the influence of the observations in the system will be larger if the observational uncertainty is smaller. From the work done until now, it is not possible to elucidate why the improvement of the scores of the experiment using pixel uncertainty exceeds those using linear model of uncertainties. One hypothesis is that the assimilation system can take advantages of this information to provide a better analysis. Another possibility is that the biases of the control run in the model and those in the SLSTR data might have opposite signs, and if the pixel uncertainty is smaller than the linear model, it could produce a better analysis only by unbiasing the DOD. However, this would cause unbalanced errors and a high risk of overfitting.

A quick look at the uncertainties provided in the level 2 product is shown in Figure 7. We have coloured three regions of this figure, showing in blue those retrievals with large AOD and large estimated uncertainty, and in orange those with large AOD but small uncertainty. When projected geographically, these colours match with the surface in the retrieval, as shown in Figure 8. Over the oceanic dust plume (and over ocean in general), the reported uncertainty is very low compared to the linear model or to those land retrievals in the domain. Given that the Godzilla dust event has large AOD values, the low relative uncertainty of the retrievals in the plume can be underestimated.

In summary, it is very likely that the low uncertainties over ocean produce an overfit in the data assimilation, that is reflected in the small-scale features of Figure 4 and some of the unexpected overestimations of the analysis DOD in the time series (peak AOD in NEON_OSBS and last days of June in Ragged Point for example).

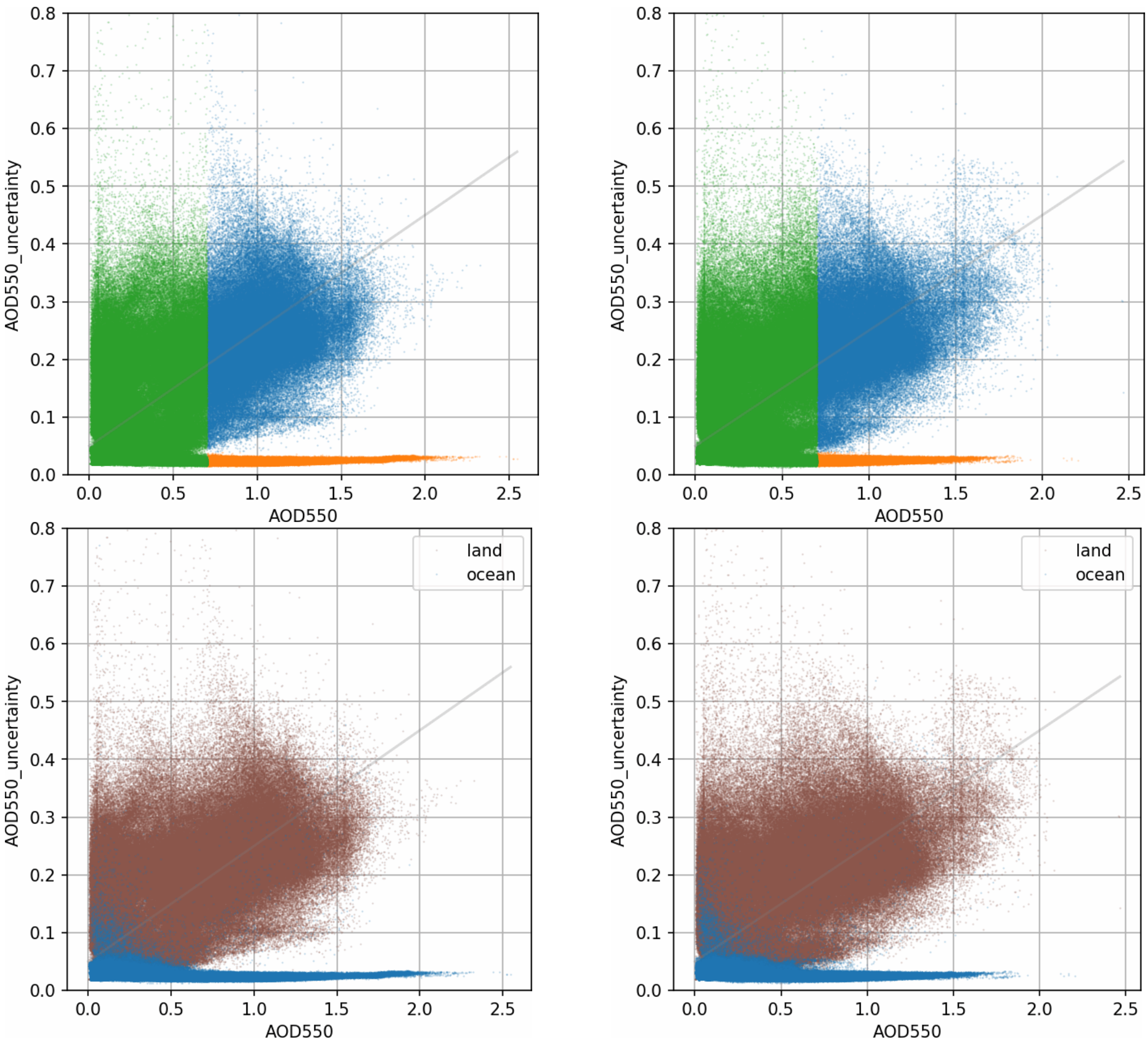

Figure 7: SLSTR AOD550 and associated uncertainties for retrievals between June 12 and June 27. Left column shows retrievals of S3A and right column shows the retrieval of S3B. For the first row, points in green have AOD<1; points in blue have AOD>0.7 and AOD

*uncertainty>0.04; while points in orange have AOD>1 and AOD uncertainty < 0.04 . Gray line shows the linear model of uncertainty 0.2*AOD+ 0.05. For the second row, same points are plotted but the blue dots are retrievals over ocean and brown dots are retrievals over land.*

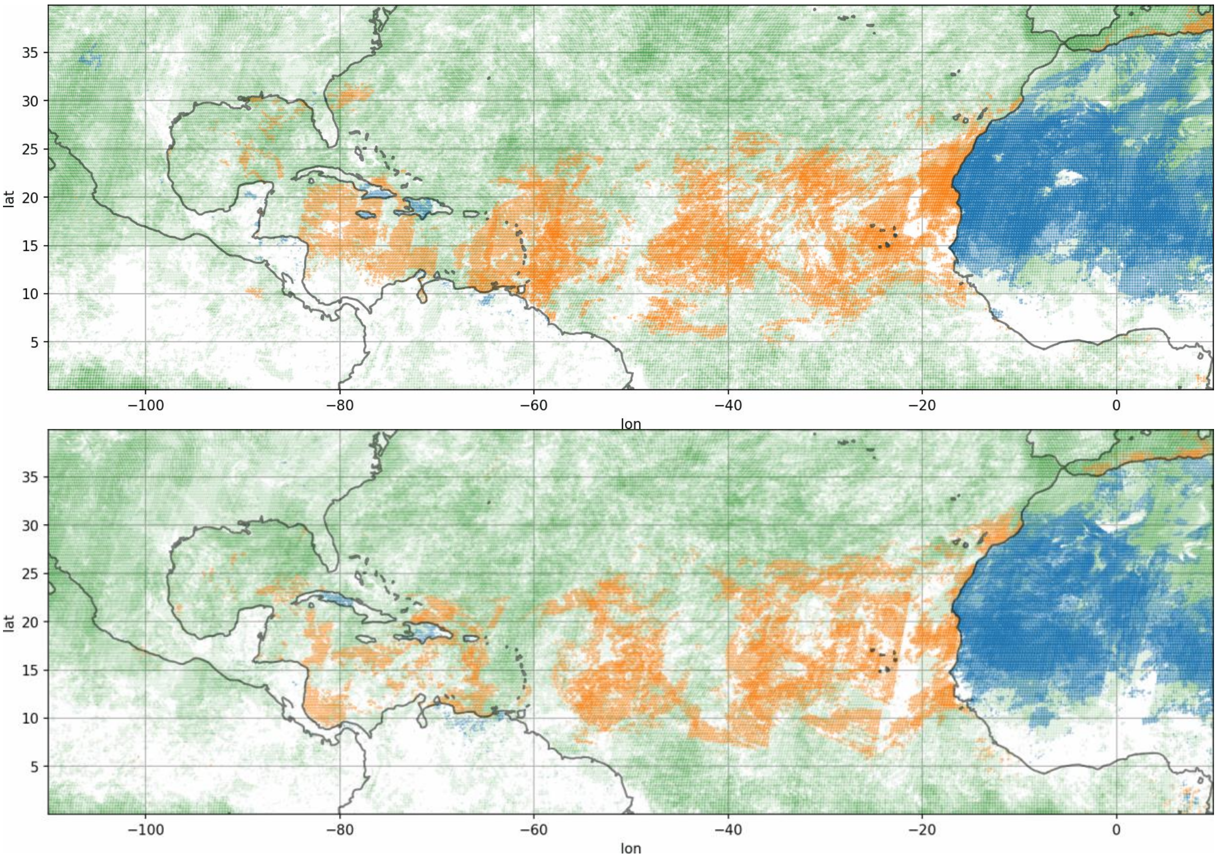

Figure 8: Geolocation of points from Figure 7. Retrievals from S3A in the upper panel, and retrievals of S3B in the lower panel

Next steps.

Despite the issue with the pixel level uncertainty, two more assimilation experiments are ongoing. In both new experiments the assimilation (and consequently the observation operator) is for coarse particles only. As in the total AOD experiments, we use both ways of defining the uncertainty, by the same linear model and by approximating the uncertainty of the coarse AOD with the uncertainty of the total AOD reported in the products. We plan also the product verifications of the (analysis-initialized) forecast skills, and not only of the analysis.

2.2. Progress on WP5.5.2 Cloud/Aerosol analysis with the ECMWF system

Lead partner: ECMWF
Authors: Kirsti Salonen and Angela Benedetti

Aim

The work package aims to implement and test Climate Change Initiative (CCI) products for aerosol optical depth (AOD) and cloud optical depth for active assimilation from the Sea and Land Surface Temperature Radiometer (SLSTR) onboard the Sentinel 3 satellites in the European Centre for Medium Range Forecasts (ECMWF) system. AOD data is provided by the Swansea University, v1.14 (personal communication P. North and K. Pearson) and COD data by Science and Technology Facilities (STFC) and Deutcher Wetter Dienst (DWD). The COD v3.3 dataset is not part of the official CCI data sets but the same algorithms are being used to cover the test periods June 2020 and September 2021 (personal communication M. Stengel and G. Thomas, 2023).

Summary of the technical preparations

By the time of the submission of the mid-term report, the focus in the work has been mainly on technical preparations to allow active assimilation of the CCI AOD and COD observations in the ECMWF system. Both data sets are provided in netCDF format. The first step is to create Observation Data Base (ODB) files from the observations. ODB is the internal data format used in the ECMWF system. The AOD and COD need their own processing chains which have been developed and implemented offline in python. The ODB files cover the 12-hour data assimilation window used in the ECMWF 4D-Var and include all quality information from the original netCDF files to allow flexible quality control in the assimilation experiments. For COD data the processing includes also re-formating the 3-dimensional (time, lat, lon) global netCDF files into 1-dimensional as the ODB was not able to handle the original format. Tables Table 2Table 2 and Table 3Table 3 summarize the variables included to the ODB files for AOD and COD, respectively.

Table 2: Summary of the variables in the AOD netCDF files and the corresponding variables in the created ODB files.

Variable name in the original netCDF file	Variable name in the ECMWF system	Variable value if constant
	reportype	98001
	groupid	99
	obstype	7
	codetype	206
	sensor	180

	distribtype	0
	seqno	0
time	date using yyyymmdd_from_epoch(time)	
time	time using hhmmss_from_epoch(time)	
latitude	lat	
longitude	lon	
AOD550	obsvalue	
	varno	174
	vertco_reference_1	0.00000055
satellite_zenith_at_center	zenith	
relative_azimuth_at_center	azimuth	
sun_zenith_at_center	solar_zenith	
surface_type_number	land_fraction	
pixel_corner_latitude1	lat_fovcorner_1	
pixel_corner_latitude2	lat_fovcorner_2	
pixel_corner_latitude3	lat_fovcorner_3	
pixel_corner_latitude4	lat_fovcorner_4	
pixel_corner_longitude1	lon_fovcorner_1	
pixel_corner_longitude2	lon_fovcorner_2	
pixel_corner_longitude3	lon_fovcorner_3	
pixel_corner_longitude4	lon_fovcorner_4	
surface_type_number	surface_type_indicator	
cloud_fraction	cloud_cover	
pixel_number	scanpos	
AOD550_uncertainty	final_obs_error	
	satellite_identifier	61 Sentinel 3A 65 Sentinel 3B

Table 3: Summary of the variables in the COD netCDF files and the corresponding variables in the created ODB files.

Variable name in the original netCDF file	Variable name in the ECMWF system	Variable value if constant
	reportype	98002
	groupid	99
	obstype	7
	codetype	206
	sensor	180

	distribtype	0
	seqno	0
yyyymmdd_from_epoch(time_desc)	date	
hhmmss_from_epoch(time_desc)	time	
lat	lat	
lon	lon	
cot_desc	obsvalue	
	varno	175
	vertco_reference_1	0.00000055
satzen_desc	zenith	
relazi_desc	azimuth	
solzen_desc	solar_zenith	
qcflag_desc	quality_retrieval	
illum_desc	surface_type_number	Note, existing ODB variable name used just for testing
cmask_desc	surface_type_indicator	Note, existing ODB variable name used just for testing
cot_desc_unc	final_obs_error	
	satellite_identifier	61 Sentinel 3A 65 Sentinel 3B

Observation operator for AODs

AOD observations from other instruments are used operationally in the ECMWF Copernicus Atmosphere Monitoring Service (CAMS) configuration so the observation operator was ready for the CCI data as well without modifications. In general, an observation operator maps the model counterpart for each observation to the observation location in space and in time. For AOD the observation operator consists of interpolating the modeled AOD from the mixing ratio value using the aerosol observation operator documented in Benedetti et al. (2009).

Observation operator for CODs

COD data is not used operationally in the ECMWF system, so implementing it has required more technical work than AOD. The ECMWF system has now been updated to allow active assimilation of COD. The observation operator is described in detail in Benedetti et al. (2008). However, it needed some technical updates to be compatible with the current operational framework but it is now tested and ready to be used in the IFS cycle 48R1. IFS documentation is available online at https://www.ecmwf.int/en/forecasts/documentation-and-support/changes-ecmwf-model/ifs-documentation .

Designing quality control and observation errors for AODs

The AOD observation quality has been evaluated in the ECMWF system with passive monitoring experiments. Passive monitoring means that the model counterpart for the observation is calculated with the corresponding observation operator but the observation has no impact in the analysis or resulting forecasts, i.e. it is passive. The monitoring experiments are a powerful way to design quality control for the new observations as well as to design realistic observation errors to be used in the active assimilation.

The data periods cover June 2020 and September 2021. Figure 9 shows the observation minus model background (OmB) bias (left panel) and standard deviation (right panel) for June 2020 over sea. In general, the data quality over sea is good, the bias is close to zero except in the tropics 75W – 80W which is related to desert dust. The bias is season dependent as can be seen in Figure 10 Figure 10 left panel where the bias is shown for September 2021. The OmB standard deviation, indicating the magnitude of random errors is also relatively homogeneous over sea except the regions where the desert dust related bias is visible.

Figures Figure 11Figure 11 (June 2020) and Figure 12Figure 12 (September 2021) show similar statistics but over land. In general, the statistics over land are more heterogeneous than over sea. The biases are season and location dependent and also the random errors are significantly higher in magnitude than over sea. Thus, at the first stage it is concluded that the active assimilation experiments should focus on data over sea only.

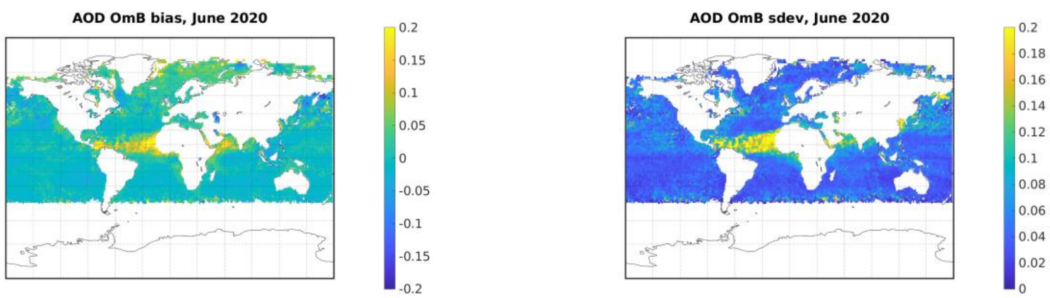

Figure 9:Observation minus model background bias (left panel) and standard deviation (right panel) for June 2020.

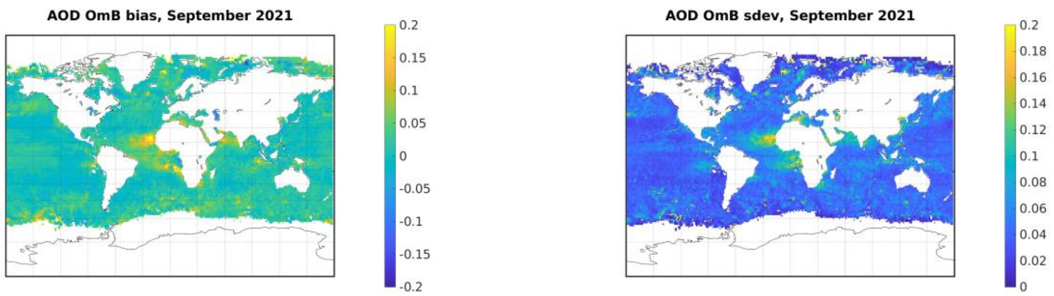

Figure 10:Similar to Figure 9 but for September 2021.

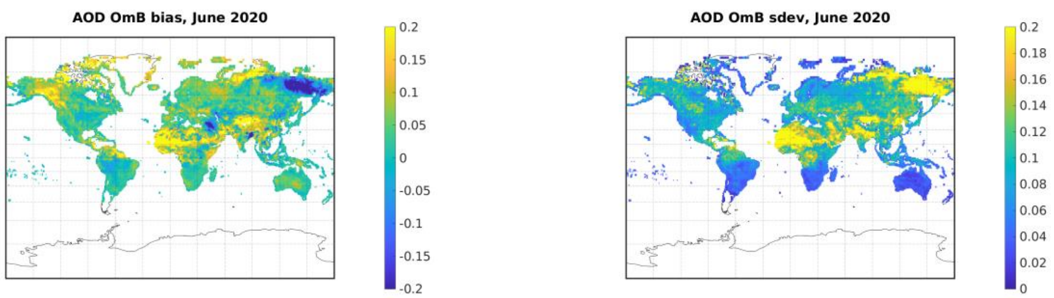

Figure 11: Similar to Figure 9 but over land.

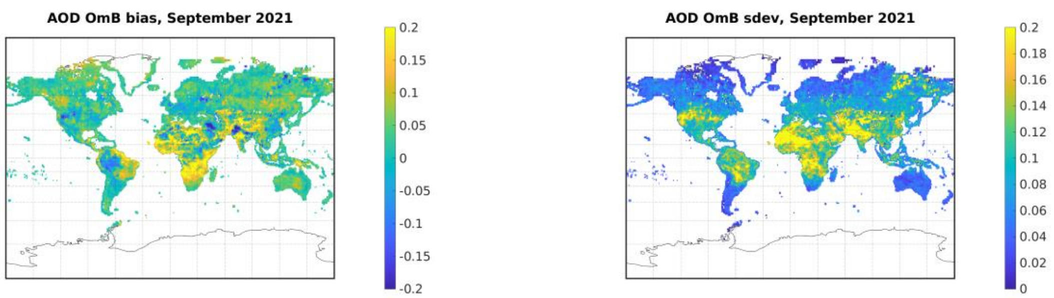

Figure 12: Similar to Figure 10 but over land.

The AOD observations are provided with uncertainty estimates. By nature, this is a scene dependent estimate of the observation error. Another estimate for the observation error is provided by the OmB standard deviation statistics. These two error estimates are compared in Figure 13Figure 13. The OmB standard deviation includes naturally also the error component of the model background. However, it is often a realistic first estimate of the magnitude of the error as there are error sources which are not explicitly taken into account in the uncertainty estimate provided, such as observation error correlations, representativeness errors or errors in the observation operator. Both of the study periods indicate that over sea the OmB standard deviation is roughly 2 times larger than the uncertainty estimate provided with AODs. This will be the first estimate for the observation errors and the impact of fine tuning the errors be will tested.

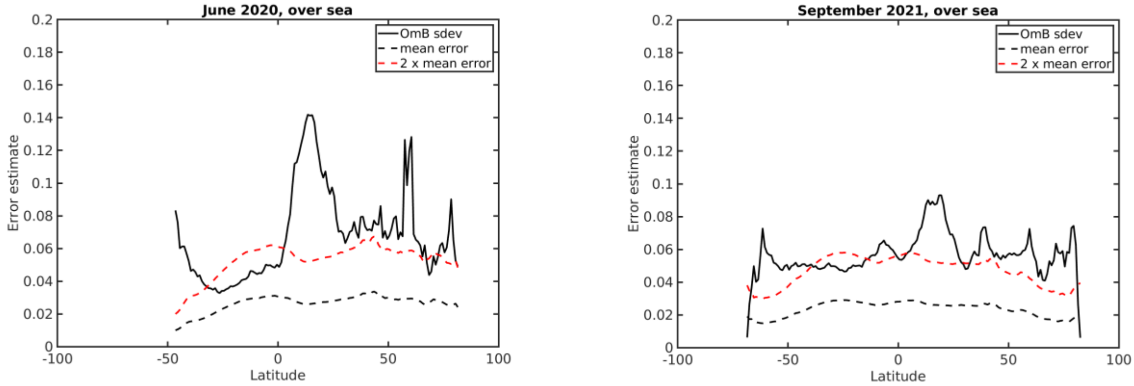

Figure 13: Zonal plot of the OmB standard deviation (black solid line), mean uncertainty estimate (black dashed line) and 2 times mean uncertainty estimate (red dashed line) for June 2020 (left panel) and September 2021 (right panel).

Next steps

The next steps will be to finalize all the technical work and perform a similar kind of passive monitoring for the COD data than has been done for AOD before moving to the active assimilation experiments. The framework for the assimilation experiments should be ready with the final fine tuning of quality control and observation errors to be tested. We plan to run the assimilation experiments both in depleted observing system (conventional observations and gps) and in full observing system. Depleted observing system experiments are helpful to show stronger impact from a new observation source but if operational implementation is considered in the future, experimentation in full observing system is of course required.

3. References

Adebiyi ,A., J.F. Kok, B.J. Murray, C.L. Ryder, J.-B.W. Stuut, R.A. Kahn, P. Knippertz, P. Formenti, N.M. Mahowald, C.P. García-Pando, M. Klose, A. Ansmann, B.H. Samset, A. Ito, Y. Balkanski, C. Di Biagio, M.N. Romanias, Y. Huang, J. Meng. A review of coarse mineral dust in the earth system Aeolian Res., 60 (2023), Article 100849, 10.1016/j.aeolia.2022.100849

Benedetti, A., and Janiskova, M.: Assimilation of MODIS cloud optical depths in the ECMWF model. Monthly Weather Review - MON WEATHER REV. 136. 10.1175/2007MWR2240.1, 2008.

Benedetti, A., Morcrette, J.-J., Boucher, O., Dethof, A., Engelen, R., Fisher, M., Flentje, H., Huneeus, N., Jones, L., Kaiser, J., Kinne, S., Mangold, A., Razinger, M., Simmons, A. J., and Suttie, M.: Aerosol analysis and forecast in the European centre for medium-range weather forecasts integrated forecast system: 2. Data assimilation, J. Geophys. Res.-Atmos., 114, D13205, https://doi.org/10.1029/2008JD011235, 2009.

Di Tomaso, E., Escribano, J., Basart, S., Ginoux, P., Macchia, F., Barnaba, F., Benincasa, F., Bretonnière, P.-A., Buñuel, A., Castrillo, M., Cuevas, E., Formenti, P., Gonçalves, M., Jorba, O., Klose, M., Mona, L., Montané Pinto, G., Mytilinaios, M., Obiso, V., Olid, M., Schutgens, N., Votsis, A., Werner, E., and Pérez García-Pando, C.: The MONARCH high-resolution reanalysis of desert dust aerosol over Northern Africa, the Middle East and Europe (2007–2016), Earth Syst. Sci. Data, 14, 2785–2816, https://doi.org/10.5194/essd-14-2785-2022, 2022.

Escribano, J., Di Tomaso, E., Jorba, O., Klose, M., Gonçalves Ageitos, M., Macchia, F., Amiridis, V., Baars, H., Marinou, E., Proestakis, E., Urbanneck, C., Althausen, D., Bühl, J., Mamouri, R.-E., and Pérez García-Pando, C.: Assimilating spaceborne lidar dust extinction can improve dust forecasts, Atmos. Chem. Phys., 22, 535–560, https://doi.org/10.5194/acp-22-535-2022, 2022.

Hunt, B. R., Kostelich, E. J., and Szunyogh, I.: Efficient data assimilation for spatiotemporal chaos: A local ensemble transform Kalman filter, Physica D, 230, 112–126, https://doi.org/10.1016/j.physd.2006.11.008, 2007.

Klose, M., Jorba, O., Gonçalves Ageitos, M., Escribano, J., Dawson, M. L., Obiso, V., Di Tomaso, E., Basart, S., Montané Pinto, G., Macchia, F., Ginoux, P., Guerschman, J., Prigent, C., Huang, Y., Kok, J. F., Miller, R. L., and Pérez García-Pando, C.: Min eral dust cycle in the Multiscale Online Nonhydrostatic AtmospheRe CHemistry model (MONARCH) Version 2.0, Geosci. Model Dev., 14, 6403–6444, https://doi.org/10.5194/gmd-14-6403-2021, 2021.

Pu, B., and Ginoux, P.: The impact of the Pacific Decadal Oscillation on springtime dust activity in Syria, Atmospheric Chemistry and Physics, 16(21), 13431-13448, 2016.